

Formation of Ge–S Bonds from AOT-Coated GeO₂ Nanoparticles at High Temperature: An in Situ Heating EXAFS Investigation

Xing Chen,^{†,‡} Quan Cai,^{†,§} Wei Wang,^{†,§} Guang Mo,^{†,§} Longsheng Jiang,^{†,§}
Kunhao Zhang,^{†,§} Zhongjun Chen,[†] Ziyu Wu,^{†,§} and Zhonghua Wu^{*,†,§}

Beijing Synchrotron Radiation Facility, Institute of High Energy Physics, CAS, Beijing 100049, China,
General Research Institute for Nonferrous Metals, Beijing 100088, China, and Graduate School of the
Chinese Academy of Sciences, Beijing 100864, China

Received November 27, 2007. Revised Manuscript Received January 24, 2008

Cubic germanium dioxide (GeO₂) nanoparticles coated by sodium bis(2-ethylhexyl) sulfosuccinate (AOT) were synthesized with a reverse micelle technique. In situ heating extended X-ray absorption fine-structure technique was used to investigate the change of the local atomic structure and electronic structure around germanium. A direct formation of Ge–S bond was found from GeO₂ at high temperature and ambient pressure. This Ge–S bond was identified to be temperature-dependent. The change of the local structure with heating is discussed. This study provides a routine process to synthesize GeS₂ from GeO₂ at higher temperature and ambient pressure.

1. Introduction

The systems based on germanium disulfide (GeS₂) have attracted extensive attention recently. Some GeS₂-based glasses have exhibited favorable electrical and optical properties. For example, Ge–Ga chalcogenide (GeS₂–Ga₂S₃) glass is a potential material for microelectronics devices.^{1,2} Bulk binary glasses, such as Ag₂S–GeS₂ or Li₂S–GeS₂ systems, are solid electrolytes with a high ionic conductivity at room temperature.^{3,4} GeO₂ and GeS₂ can be used as precursors⁵ to form thiogermanic acids under a rigorous high-temperature and high-pressure condition. Indeed, GeS₂ is a good glass former and shows noble electronic and optical properties as well as potential applications in these areas of fast ion conducting glass for battery applications,^{6–8} hologram recording media, optical coatings, fiber optics, and semiconductors and hydrogen fuel cell membranes,^{9–12} and so on. However, germanium disulfide was commonly synthe-

sized with high-temperature treating germanium and sulfur¹³ under vacuum or sol–gel approach.¹⁴ Because of the wide application of germanium disulfide, new approaches to synthesize GeS₂ are attractive. Specifically, synthesizing GeS₂ directly from GeO₂ is economical. Up to now, there are hardly any research reports about the GeS₂ synthesis with GeO₂ as starting materials.

In this paper, GeO₂ nanoparticles were first prepared. In situ heating extended X-ray absorption fine structure (EXAFS) technique was used to inspect the structural change around germanium atoms. Unexpectedly, GeO₂ has been completely transformed into GeS₂ at high temperature. The synthesis of GeS₂ directly from GeO₂ at high temperature and ambient pressure has been investigated. Although the formation mechanism is not very clear, the approach to synthesize the GeS₂ from GeO₂ is still significant in practical application.

2. Experimental Section

Sample Preparation. The details of the sample preparation were described in elsewhere.¹⁵ Sodium bis(2-ethylhexyl) sulfosuccinate (AOT) and GeCl₄ (99.999%) were purchased from Aldrich. Isooctane with analytical grade was obtained from Beijing chemicals. All reagents were used without further purification. In a typical synthesis procedure, 0.88 g of AOT was dissolved in 40 mL of isooctane and stirred for 0.5 h to form a transparent solution. Then the solution was divided into two parts, and 25.5 μ L of GeCl₄ and the corresponding water (the volume based on the molar ratio of water/AOT) were added into the two parts of the solution, respectively. After the solutions were stirred for 1 h,

* Corresponding author. E-mail: wuzh@ihep.ac.cn.

[†] CAS.

[‡] General Research Institute for Nonferrous Metals.

[§] Graduate School of the Chinese Academy of Sciences.

- (1) Julien, C.; Barnier, S.; Massot, M.; Chbani, N.; Cai, X.; Lozach, A. M. L.; Guittard, M. *Mater. Sci. Eng., B* **1994**, *22*, 191.
- (2) Fontana, M.; Rosi, B.; Ivanova, Z.; Kirov, N. *Philos. Mag. B* **1987**, *56*, 507.
- (3) Souquet, J.; Robinel, E.; Barrau, B.; Ribes, M. *Solid State Ionics* **1981**, *3*, 317.
- (4) Pradel, A.; Ribes, M. *Mater. Chem. Phys.* **1989**, *23*, 121.
- (5) Sutherland, J. T.; Poling, S. A.; Nelson, C. R.; Martin, S. W. *Solid State Ionics* **2004**, *175*, 703.
- (6) Martin, S. J. *Am. Ceram. Soc.* **1991**, *74*, 1767.
- (7) Martin, S. J. *Non-Cryst. Solids* **1986**, *83*, 185.
- (8) Poling, S.; Sutherland, J.; Nelson, C.; Martin, S. J. *Phys. Chem. B* **2003**, *107*, 5413.
- (9) Poling, S.; Sutherland, J.; Nelson, C.; Martin, S. *Solid State Ionics* **2004**, *170*, 43.
- (10) Simons, D. R.; Faber, A. J.; Dewaal, H. J. *Non-Cryst. Solids* **1995**, *185*, 283.
- (11) Marchese, D.; Kakarantzas, G.; Jha, A.; Samson, B. N.; Wang, J. J. *Mod. Optics* **1996**, *43*, 963.
- (12) Haase, M.; Bechtel, H.; Czarnojan, W.; Waedow, D. *Chem. Abstr.* **1996**, *125*, 99556v. (Philips Electronics N.V., EP-B 714 966, 1996).

(13) Shimada, M.; Dachille, F. *Inorg. Chem.* **1977**, *16*, 2094.

(14) Seddon, A. B.; Hodgson, S. N. B.; Scott, M. G. *J. Mater. Sci.* **1991**, *26*, 2599.

(15) Chen, X.; Cai, Q.; Zhang, J.; Chen, Z. J.; Wang, W.; Wu, Z. Y.; Wu, Z. H. *Mater. Lett.* **2007**, *61*, 535.

transparent AOT/water/isooctane solution was added to the AOT/ GeCl_4 /isooctane solution to form a mixture solution. Then, the isooctane in the mixture solution was volatilized at 70 °C in air. The residue was annealed at 250 °C for 2 h to remove partially the surfactant AOT and was collected as the as-prepared sample and marked as Ge025. In the above sample preparation, AOT is not absolutely necessary for the second solution of AOT/ GeCl_4 /isooctane. In addition, in order to exclude the chlorine from the starting materials, germanium tetraoxide, instead of GeCl_4 , was also used as a starting material, and spherical GeO_2 nanoparticles 50 nm in diameter were synthesized with a similar method.

XRD, TEM, and EXAFS Measurement. The transmission electron microscopy (TEM) micrograph and X-ray diffraction (XRD) pattern of the sample have been published in elsewhere.¹⁵ TEM micrographs demonstrated that the nanoparticles in sample Ge025 are in cubic shape with particle size of about 15 nm. The X-ray diffraction (XRD) pattern identified that the as-prepared sample has the same crystalline structure as α -quartz GeO_2 . In this study, sample Ge025 was pressed into a pill with an optimized absorption thickness ($\Delta\mu d \approx 1.0$). In situ heating EXAFS measurements for sample Ge025 were performed at EXAFS station (beam line 1W1B) of BSRF in transmission mode. The storage ring was run at 2.2 GeV with an average electron current of 80 mA. The incident X-ray was monochromatized by a double-crystal Si(111) monochromator. The as-prepared sample Ge025 was, respectively, heated with a heating rate of 8 °C/min to 200 °C, 300 °C, 400 °C, 500 °C, 600 °C, and 700 °C. After 1/2 h of heat-preservation at each target temperature, its EXAFS spectrum was collected and denoted as Ge200, Ge300, Ge400, Ge500, Ge600, and Ge700, respectively. All these target temperatures were stabilized within ± 2 °C. Finally, the sample was quenched to room temperature from 700 °C, and 20 h later its EXAFS spectrum was collected and denoted as qu-Ge025. The spherical GeO_2 nanoparticles coated by AOT were also heated to 600 °C for collecting the EXAFS spectrum at beamline 10B of the Photon Factory and marked as sph-Ge600. In the in situ heating EXAFS experiments, the heating furnaces used for the cubic and spherical GeO_2 nanoparticles are slightly different. The X-ray entrance window and exit window of the heating furnace used at BSRF was sealed using a Kapton film but left a small hole to maintain the atmospheric pressure, whereas the X-ray entrance window and exit window of the heating furnace used at Photon Factory was completely open to air.

TG-DTA Characterization. In order to realize the thermal effect in the heating process of the as-prepared GeO_2 nanoparticles, thermogravimetric analysis (TG) and differential thermal analysis (DTA) were used to detect their possible thermal behaviors. Although the as-prepared sample Ge025 had been heat-treated at 250 °C for 2 h before TG and DTA measurements, the coating of surfactant AOT will possibly exist on the surface of the GeO_2 nanoparticles. Or there may be some AOT residual ligands remaining in Ge025. In order to simulate the thermal decomposition of AOT in the as-prepared Ge025, pure surfactant AOT was also heated at 250 °C for 2 h as done for the as-prepared

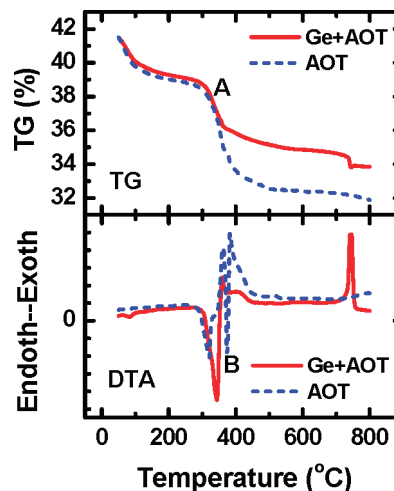


Figure 1. Comparison of TG and DTA curves for the as-prepared sample Ge025 and surfactant AOT.

sample. Then, this surfactant AOT was used to do thermogravimetric analysis and differential thermal analysis. Its TG and DTA curves are compared with that of Ge025 as shown in Figure 1.

3. EXAFS Data analysis

X-ray absorption-near-edge structure (XANES) and EXAFS spectra of Ge K-absorption were analyzed with WinXAS3.1.¹⁶ The energy threshold was calibrated to the maximum of the first derivative of the absorption spectra. After removing the pre-edge background and normalizing the absorption spectra, EXAFS signals were extracted by subtracting a postedge background obtained with a cubic spline-fit. These EXAFS signals from 2.0 to 14.2 Å⁻¹ were Fourier transformed into R-space with a k^3 -weight. Then, the near-neighbor EXAFS spectra can be isolated from the Fourier transform spectra. Bessel window was always used in both the Fourier transform and Fourier filter. The k^3 -weight EXAFS spectra were fitted with least-squares refinement.¹⁷ Based on the crystalline structures of α -quartz type GeO_2 (q- GeO_2)¹⁸ and α - GeS_2 ,¹⁹ the reference amplitudes and phase shifts of Ge—O and Ge—S bonds were calculated with FEFF7 code.^{20,21}

4. Results and Discussion

TG-DTA Analysis. TG and DTA curves of the as-prepared sample Ge025 with AOT residue are compared with those of the pure surfactant AOT annealed at 250 °C as shown in Figure 1. Three different courses can be found from Figure 1. First, The TG curves demonstrate that the adsorbed water is evaporated below 100 °C. Second, by comparing the TG and DTA curves between GeO_2 and AOT, it can be

(16) Ressler, T. J. *J. Synchrotron Radiat.* **1998**, *5*, 118.

(17) Sayers, D. E.; Stern, E. A.; Lytle, F. W. *Phys. Rev. Lett.* **1971**, *27*, 1204.

(18) Yamanaka, T.; Ogata, K. *J. Appl. Crystallogr.* **1991**, *24*, 111–118.

(19) Dittmar, G.; Schaefer, H. *Acta Crystallogr., Sect. B* **1976**, *32*, 1188.

(20) Ankudinov, A. L.; Ravel, B.; Rehr, J. J.; Conradson, S. D. *Phys. Rev. B* **1998**, *58*, 7565.

(21) Ankudinov, A. L.; Bouldin, C.; Rehr, J. J.; Sims, J.; Hung, H. *Phys. Rev. B* **2002**, *65*, 104107.

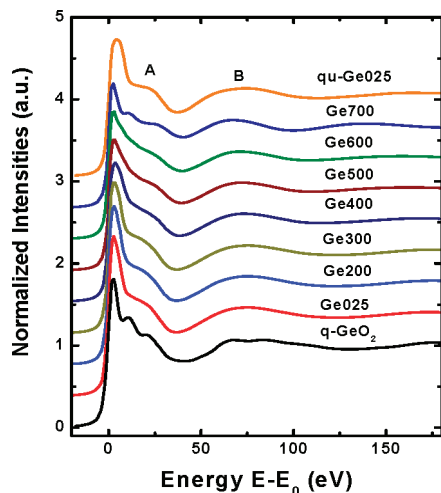


Figure 2. Normalized Ge K-edge XANES spectra with different in situ heating temperatures.

found that the surfactants AOT are decomposed around 300 °C. The similar thermogravimetric and differential thermal behaviors between GeO₂ and AOT indicate indeed that there are some residues of AOT remaining on the surface of the as-prepared GeO₂ nanoparticles after 2 h of heating at 250 °C. With the temperature increasing, the residual AOT is gradually decomposed and burnt off. But at about 380 °C, a knee A in the TG curve of GeO₂ is probably corresponding to desorption of the AOT residues from the GeO₂ nanoparticles. A modicum of sag is also presented on the DTA curve of GeO₂ nanoparticles at about the same temperature. These imply that the surfactant AOT was partially adsorbed on the surface of GeO₂ nanoparticles in the sample preparation. An endothermic peak B in the DTA curve of AOT corresponds possibly to the breakdown of the Na–S bonds in AOT. Finally, a sharp exothermic peak at about 700 °C can be found from the DTA curve of the GeO₂ nanoparticles. This peak does not appear on the DTA curve of AOT, illustrating that it is irrespective of the AOT. This exothermic peak can be attributed to the reaction between GeO₂ and the sulfide which was formed from the decomposition of the surfactant AOT. In such a reaction, the Ge–O bonds in the GeO₂ nanoparticles have been replaced by the Ge–S bonds. This bond change will be confirmed again by the in situ heating EXAFS measurement and will be discussed later.

XANES Spectra. Normalized Ge K-edge XANES spectra with different in situ heating temperatures are shown in Figure 2. The main peaks correspond to the electron transition from 1s to 4p. Feature A reflects the chemical environment around central Ge atom. It can be seen from Figure 2 that features A in Ge025, Ge200, and Ge300 are very similar, indicating the similarity of their local atomic structure. With temperature increasing, feature A becomes gradually expanate. Up to 700 °C, feature A is split into two kinks. The two kinks in Ge700 are somewhat similar with the two peaks in q-GeO₂, but their positions are not completely the same. The change of feature A indicates that the local and electronic structures at 700 °C around Ge are different from the others, which suggests that a new structure probably occurs. The high-energy features B can be attributed

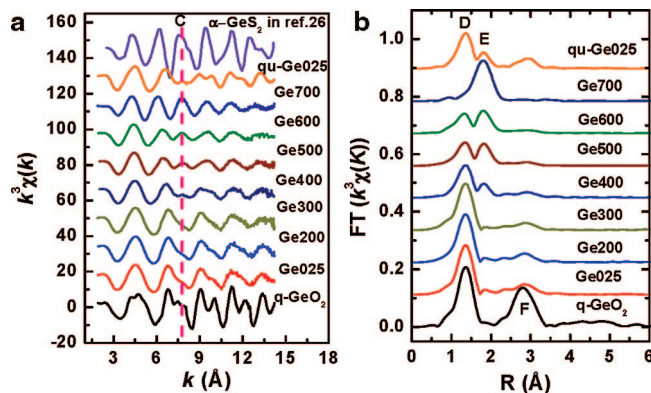


Figure 3. (a) Ge K-edge k^3 -weighted EXAFS signals (left panel) and (b) the corresponding FT spectra (right panel).

to multiple scattering inside the first shell.²² Feature B shifts toward low energy with temperature increasing, indicating an increase of bond length in the first coordination shell.²³

EXAFS Spectra. The k^3 -weighted EXAFS signals and their FT spectra are compared in Figure 3. Before further data analysis, we can conclude that these GeO₂ nanoparticles have almost the same local atomic structures when the in situ heating temperature is lower than 400 °C. Starting from 400 °C, a new signal marked as C appears on the EXAFS oscillations as shown in Figure 3a, and this new signal is from strong to strong until 700 °C. Simultaneously, the EXAFS-oscillation frequency increasing with temperature indicates the bond-length elongation, which is well consistent with the XANES features. A similar trend is repeated on the FT spectra as shown in Figure 3b. From room temperature to 300 °C, the local coordination peaks around central Ge atom are almost the same. As the temperature is higher than 300 °C, a new coordination shell (peak E) at the higher R side appears, and it becomes dominant with temperature increasing. Up to 700 °C, the new coordination peak replaces completely the original coordination peak which is corresponding to the Ge–O contribution. For the new coordination peak E, we can exclude the possibility of the thermal expansion²⁴ or the phase transition from the q-GeO₂ structure to the rutile-type GeO₂ (r-GeO₂) structure.^{18,25} Actually, this new coordination peak is from the Ge–S contribution, which will be further discussed. Evidently, the contribution of Ge–O bonds decreases and the contribution of Ge–S bonds increases with temperature increasing. This change is in good agreement with those indicated by TG-DTA and XANES results.

By comparing the EXAFS oscillations and the FT spectra between the GeO₂ nanoparticles with temperature lower than 400 °C and the q-GeO₂ bulk at room temperature, it is credible that these samples have similar local atomic

(22) Wu, Z. Y.; Jollet, F.; Seifert, F. J. *Phys.: Condens. Matter* **1998**, *10*, 8083.

(23) Natoli, C. R. In *EXAFS and Near Edge Structure*; Springer Series in Chemistry and Physics; Bianconi, A., Incoccia, L., Stipcich, S., Eds.; Springer: Berlin, 1983; Vol. 27, p 43.

(24) Haines, J.; Cambon, O.; Philippon, E.; Chapon, L.; Hullz, S. J. *Solid State Chem.* **2002**, *166*, 434.

(25) Bolzan, A. A.; Fong, C.; Kennedy, B. J.; Howard, C. J. *Acta Crystallogr., Sect. B* **1997**, *53*, 373.

structures except for the second coordination peak F in the FT spectra or finer structures at EXAFS oscillation. A new phase began forming at 400 °C and was matured at 700 °C. In order to illustrate the structural change, a $k^3\chi(k)$ function²⁶ of α -GeS₂ cited from ref 26 is also shown in Figure 3a. Obviously, the EXAFS oscillations of Ge700 and α -GeS₂ have the same frequency except for the weaker amplitude and the absence of the fine structure in Ge700. This implies that the local atomic structures between Ge700 and α -GeS₂ are similar. Combining the change shown in the FT spectra, we think that the new coordination structure (peak E) is from the Ge–S bond and forms a GeS₂-like new phase. This will be further confirmed by the EXAFS data analysis.

It is a bit surprising to find that Ge700 is so different from the as-prepared sample. We took it for granted that this high temperature phase could be preserved at room temperature by quenching Ge700 to low temperature. However, this attempt failed because of the conversion from the Ge–S bond to the Ge–O bond. Quenching is nonequilibrium thermodynamics, and it is frequently used to preserve the metastable high temperature phase at room temperature. If the high temperature phase was slowly cooled to room temperature, it is out of question that the Ge–S bond would be completely transformed back to the Ge–O bond at the presence of sufficient oxygen and obtained a stable GeO₂ phase. In order to stop the phase transition from the Ge–S bond to the Ge–O bond and get the GeS₂ new phase at room temperature, excluding oxygen from the high-temperature sample is necessary during the sample cooling. Therefore, for the high temperature phase to be useful at room temperature, a possible method is to cool the sample under vacuum or without the presence of oxygen. For this purpose, a further study is needed in the future for the stability of this Ge–S bond and the corresponding chemical reaction.

Figure 3 shows also the room-temperature EXAFS spectrum of the quenching sample (qu-Ge025). It can be seen that the quenching sample has almost the same spectral characteristics with sample Ge400 except a better signal-to-noise ratio because of the increase of particle size and the decrease of the thermal disorder. This clearly tells us that the conversion from GeO₂ to GeS₂ (Ge–S bond in Ge700) is reversible in the presence of sufficient oxygen. At high temperature, the Ge–S bond is stable, but the Ge–O bond is stable at lower temperature. By comparing the FT spectra of these nanoparticles with that of bulk q-GeO₂, the coordination peaks D and F can be attributed to Ge–O and Ge–Ge contributions, respectively. The lower magnitudes of the Ge–Ge coordination peaks in these in situ heating nanoparticles are due to the small particle sizes and larger thermal disorder. Especially for Ge700, only the nearest Ge–S coordination peak can be observed in Figure 3b, and no higher-shell peaks appear. This demonstrates that the high-temperature phase is in an amorphous state, only having the short-range-order structure.

To confirm further that peak E is from the Ge–S bonds, the following tests were performed. First, because the Ge–O coordination was used to fit the first coordination peak E of

Table 1. Structural Parameters of the First Coordination Peak in Sample Ge700, which Were Obtained by Fitting the First-Shell EXAFS Oscillations with Ge–Cl and Ge–S Bonds, Respectively

sample	bonds	N	R (Å)	σ^2 (Å ² , $\times 10^{-3}$)	ΔE_0 (eV)
Ge700	Ge–S	3.9 \pm 0.5	2.22 \pm 0.01	7.5 \pm 2.5	5.6 \pm 1.5
	Ge–Cl	3.6 \pm 0.4	2.21 \pm 0.01	7.8 \pm 2.5	7.6 \pm 2.4

Ge700, the fitting parameters are not reliable and the fitting qualities are not acceptable, so the contribution from the Ge–O bonds can be excluded out of the first coordination peak E of sample Ge700. Second, Lewis et al. reported a direct formation of Ge–C bonds from GeO₂. Although the formation mechanism is unknown, they ruled out the participation from CO, H₂, or carbon.²⁷ Therefore, it was also attempted to fit the Ge–C bonds to the first coordination peak of sample Ge700, but it failed. Obviously, the Ge–C contribution can be also excluded from the first coordination peak. Third, according to sample preparation and the starting materials or the byproduct, there are still two possibilities referenced to the coordination peak E. That is to say, the chlorides or sulfides may react with GeO₂ to displace the Ge–O bonds with Ge–Cl or Ge–S bonds. Therefore, Ge–Cl and Ge–S bonds were, respectively, used to fit the coordination peak E of Ge700. The fitting parameters are listed in Table 1.

In point of the EXAFS spectral fitting, both Ge–Cl bonds and Ge–S bonds are all acceptable for the local atomic coordination in sample Ge700. There are about 3.9 S-atoms surrounding Ge with a bond length of 2.22 Å or 3.6 Cl-atoms surrounding Ge with a bond length of 2.21 Å. That is to say, we cannot distinguish the Ge–S or Ge–Cl bonds on the basis of the goodness of fit. However, it is well-known that germanium halides were commonly synthesized through the chemical reaction between elemental germanium and hydrogen chloride or aryl halides with copper catalyst^{28,29} or without catalyst.³⁰ Although Huang et al.³¹ also claimed theoretically that GeO₂ can react with NaCl to form GeCl₄ at high temperature in the presence of SO₂, we know that the boiling point of GeCl₄ is 83 °C and it cannot exist steadily in air. At the same time, if we guess that the Ge centers are surrounded by Cl atoms in sample Ge700, then the Ge–Cl bond length of 2.21 Å in Ge700 is remarkably larger than that (2.09 Å) in GeCl₄. Obviously, this hypothesis seems inappropriate.

In order to judge the chemical bonding species around Ge in sample Ge700, the XANES spectrum of Ge700 and that³² of GeCl₄ cited from ref 32 are compared in Figure 4. It can be seen that the XANES features are not identical between Ge700 and GeCl₄. However, the EXAFS spectral charac-

(26) Armand, P.; Ibanez, A.; Dexpert, H.; Philippot, E. *J. Non-Cryst. Solids*, **1992**, 139, 137.

(27) Lewis, L. N.; Litz, K. E.; Anostario, J. M. *J. Am. Chem. Soc.*, **2002**, 124, 11718.
 (28) (a) Rochow, E. G. *J. Am. Chem. Soc.* **1947**, 69, 1729. (b) Moedritzer, K. *J. Organomet. Chem.* **1966**, 6, 282.
 (29) Rochow, E. J. *J. Am. Chem. Soc.* **1950**, 72, 198. Rochow, E. G.; Didtschenko, R.; West, R. C., Jr. *J. Am. Chem. Soc.* **1951**, 73, 5486.
 (30) Rochow, E. G.; Abel, E. W. In *The Chemistry of Germanium, Tin and Lead*, Pergamon; Oxford, U.K., 1973. Dennis, L. M.; Orndorff, W. R.; Tabern, D. L. *J. Phys. Chem.* **1926**, 30, 1049.
 (31) Zhang, Y. F.; Wang, H. F.; Huang, B. F. *J. Guizhou Univ. Technol.* **2001**, 30, 13.
 (32) Bouldin, C. E.; Bunker, G.; Mckeown, D. A.; Forman, R. A.; Ritter, J. J. *Phys. Rev. B* **1988**, 38, 10816.

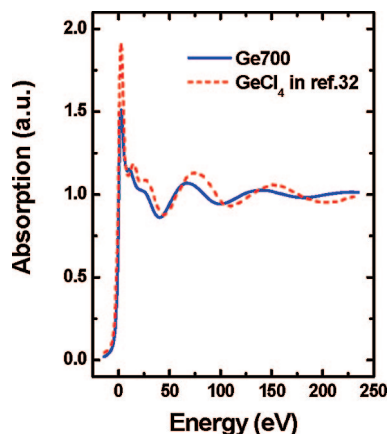


Figure 4. Ge K-edge XANES comparison between Ge700 and GeCl₄ cited from ref 32.

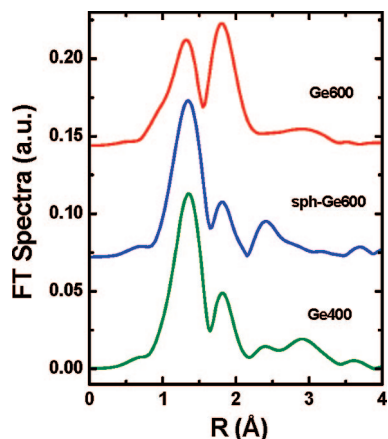


Figure 5. Comparison of the Ge K-edge FT spectra among sph-Ge600, Ge400, and Ge600.

teristic of Ge700 is quite similar with that of α -GeS₂,¹⁹ having the same oscillation frequency. This confirms that the Ge atoms are bonded to sulfur, instead of chlorine in sample Ge700. In addition, Ge K-edge EXAFS spectrum of sph-Ge600 was also collected at 600 °C. The Fourier transformed spectra of sph-Ge600, Ge400, and Ge600 are compared in Figure 5. In the preparation of spherical GeO₂ nanoparticles (sph-Ge600), the element chlorine was completely excluded from the starting materials. Therefore, the Ge–Cl bonds will never appear in this sample in any case. However, peak E appears again on the FT spectrum of sph-Ge600, which confirms again that peak E is corresponding to the contribution of the Ge–S bond.

α -GeS₂¹⁹ is a high temperature phase, in which Ge occupies six different crystal lattice sites. Each germanium atom is coordinated with four sulfur atoms and locates at the center of the slightly distorted sulfur tetrahedron. The Ge–S bond lengths are distributed in the range of 2.169–2.287 Å with an averaged value of 2.22 Å. The average structure around Ge in α -GeS₂ is almost the same with the local atomic structures of Ge in Ge700 as obtained by fitting the EXAFS signal with Ge–S bonds. Besides all these, in the high-temperature and high-pressure synthesis of H₂Ge₄S₉ and H₄Ge₄S₁₀ with starting materials of GeO₂ and H₂S, it was confirmed that a small quantity of α -GeS₂ can be formed as the reaction byproduct.¹² This demonstrates that germanium

sulfide can be synthesized from GeO₂ under some appropriate reaction conditions. Therefore, we believe that Ge700 is a GeS₂-like structure. The nearest near neighbors around Ge in Ge700 are sulfur atoms. The germanium sulfide has been successfully synthesized in the high temperature without high pressures. And, it can be seen that almost all Ge–O bonds are displaced by Ge–S bonds at 700 °C as shown in Figure 3b. This reaction from the Ge–O bond to the Ge–S bond is thorough, and almost all GeO₂ nanoparticles have been completely transformed to the GeS₂-like phase in this study.

Although sph-Ge600 and Ge600 were heated to the same temperature (600 °C), the conversion ratio from Ge–O bonds to Ge–S bonds is different. Obviously, more Ge–O bonds had been displaced by Ge–S bonds in Ge600 than in sph-Ge600 as shown in the FT spectra in Figure 5. The content of the Ge–S bonds is even slightly less in sph-Ge600 than in Ge400. This difference of conversion ratio between sph-Ge600 and Ge600 demonstrates that the reaction rate is dependent not only on the temperature but also on the particle size. The smaller the particle size or the higher the temperature, the easier the reaction is. In the chemical reaction from Ge–O bonds to Ge–S bonds, GeO₂ nanoparticles play a part of the self-catalysis.

To confirm further the change of the local atomic structure around germanium, the nearest near-neighbor EXAFS signals were isolated from the FT spectra in the range of 0.8–2.2 Å. The best fitting parameters are listed in Table 2. An asymmetrical Ge–O atom-pair model with the third cumulant $\delta^{(3)}$ was used to fit the EXAFS curves of Ge025, Ge200, and Ge300. There are about four oxygen atoms coordinated to germanium, illustrating that GeO₂ nanoparticles have the similar Ge coordination configuration with quartz-type GeO₂, but the Ge–O distance of 1.79 Å as listed in Table 2 is slightly larger than the Ge–O bond length of 1.74 Å in crystalline bulk q-GeO₂. This is because the small particle size and the large ratio of surface to volume induce the Ge–O bond elongation.

With the heating temperature increasing, a new phase of germanium sulfide appears, and the two Ge–O and Ge–S subshells were used to fit the coordination peaks D and E, respectively. The best fitting curves are shown in Figure 6. Indeed, the Ge–O coordination number decreases and the Ge–S coordination number increases with temperature increasing. There are only four Ge–S bonds located at 2.22 Å in sample Ge700 without Ge–O contribution. As sample Ge700 was quenched to room temperature and stood for 48 h in air, its near neighbor EXAFS curve is very similar to that of Ge400. Oxygen atoms reappear at the near neighbor of germanium and become the dominant component. This illustrates that this Ge–S bond is not stable at room temperature. The phase transition from Ge–O to Ge–S is reversible in the presence of sufficient oxygen. Seddon et al.³³ reported also that GeS₂ can be slowly hydrolyzed into oxide at room temperature with exposure to water. It is in good agreement with our observation in this study.

Finally, the formation mechanism of GeS₂ is simply discussed as follows. In the sample preparation, GeO₂

(33) Seddon, A. B.; Hodgson, S. N. B.; Scott, M. G. *J. Mater. Sci.* **1991**, *26*, 2599.

Table 2. Structural Parameters of the in Situ Heating AOT-Coated GeO₂ Nanoparticles^a

sample	bonds	<i>N</i>	<i>R</i> (Å)	σ^2 (Å ² , × 10 ⁻³)	ΔE_0 (eV)	$\sigma^{(3)}$ (Å ³ , × 10 ⁻⁴)
q-GeO ₂	Ge—O	4.0	1.74	2.5	5.0	
Ge025	Ge—O	4.3 ± 0.5	1.79 ± 0.01	4.3 ± 1.5	6.7 ± 3.5	3.7 ± 3.1
Ge200	Ge—O	4.3 ± 0.5	1.79 ± 0.01	4.4 ± 2.3	6.7 ± 3.8	3.4 ± 3.3
Ge300	Ge—O	4.2 ± 0.5	1.80 ± 0.01	4.6 ± 2.5	7.1 ± 3.6	3.7 ± 3.2
Ge400	Ge—O	2.8 ± 0.4	1.78 ± 0.01	4.3 ± 2.1	6.3 ± 3.1	
	Ge—S	1.3 ± 0.3	2.15 ± 0.01	6.9 ± 2.8	3.6 ± 2.5	
Ge500	Ge—O	2.3 ± 0.4	1.78 ± 0.01	4.9 ± 2.5	5.6 ± 2.6	
	Ge—S	1.9 ± 0.4	2.18 ± 0.01	6.8 ± 2.3	5.7 ± 2.6	
Ge600	Ge—O	1.9 ± 0.4	1.77 ± 0.01	5.1 ± 1.6	4.9 ± 3.5	
	Ge—S	2.2 ± 0.4	2.19 ± 0.01	8.1 ± 2.5	5.1 ± 3.2	
Ge700	Ge—S	3.9 ± 0.5	2.22 ± 0.01	7.7 ± 3.2	5.6 ± 3.5	
qu-Ge025	Ge—O	2.6 ± 0.5	1.78 ± 0.01	3.1 ± 2.5	5.6 ± 3.5	
	Ge—S	1.5 ± 0.3	2.14 ± 0.01	6.6 ± 2.5	1.5 ± 1.5	

^a Ge025, Ge200, Ge300, Ge400, Ge500, Ge600, and Ge700 denote the sample was heated to 25 °C, 200 °C, 300 °C, 400 °C, 500 °C, 600 °C, and 700 °C, respectively. qu-Ge025 denotes the sample was quenched to room temperature from 700 °C. q-GeO₂ is the α-quartz type GeO₂ at room temperature.

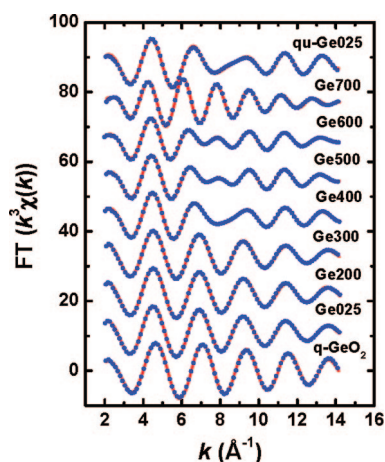
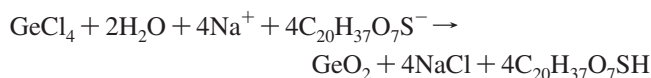


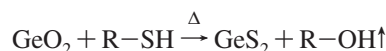
Figure 6. Ge K-edge EXAFS functions with k^3 -weight. Solid line is the experimental curves, dashed line is the fitting results.

nanoparticles was first synthesized according to the following chemical reaction:¹⁵



A similar chemical reaction of GeCl_4 with sodium tetraethoxide (Na(OEt)_4) to form Ge(OEt)_4 and NaCl was also reported by Johnson and Fritz.³⁴ In the as-prepared sample, surfactant AOT forms a coating shell adsorbed on the surface of GeO_2 nanoparticles. As the sample was heated, surfactant

AOT was decomposed and left the residual ligands, which are denoted as R-SH . At an appropriate temperature, the following chemical reaction could be performed:



Obviously, the small size of the GeO_2 nanoparticles is propitious to this chemical reaction. This study provides a routine process to synthesize GeS_2 from GeO_2 .

5. Conclusion

In situ heating EXAFS study on the AOT-coated GeO_2 nanoparticles was performed. The local atomic structures around the Ge atom have been determined. A direct formation of the Ge—S bonds from AOT-coated GeO_2 nanoparticles at ambient pressure is first found. With increasing temperature, the Ge—O bonds can be replaced gradually by Ge—S bonds. At about 700 °C, GeO_2 can be completely transformed into GeS_2 . But this GeS_2 is an amorphous phase with α- GeS_2 -like short-range-order structure and is only stable at high temperature. The conversion from GeO_2 to GeS_2 is reversible at the presence of sufficient oxygen. This study indicates a new approach to synthesize GeS_2 .

Acknowledgment. The work is supported by the National Natural Science Foundation of China with No. 10374087 and the Knowledge Innovation Program of the Chinese Academy of Sciences (KJCX3-SYW-N8).

(34) Johnson, O. H.; Fritz, H. E. *J. Am. Chem. Soc.* **1953**, 75, 718.